PHYSICAL REVIEW A **81**, 010702(R) (2010)

Large spin relaxation rates in trapped submerged-shell atoms

Colin B. Connolly,[1,3] Yat Shan Au,[1,3] S. Charles Doret,[1,3] Wolfgang Ketterle,[2,3] and John M. Doyle[1,3]
[1]*Department of Physics, Harvard University, 17 Oxford Street, Cambridge, Massachusetts 02138, USA*
[2]*Department of Physics, Massachusetts Institute of Technology, Cambridge, Massachusetts 02139, USA*
[3]*Harvard-MIT Center for Ultracold Atoms, Cambridge, Massachusetts 02138, USA*
(Received 20 August 2009; published 20 January 2010)

Spin relaxation due to atom–atom collisions is measured for magnetically trapped erbium and thulium atoms at a temperature near 500 mK. The rate constants for Er–Er and Tm–Tm collisions are 3.0×10^{-10} and 1.1×10^{-10} cm^3 s^{-1}, respectively, 2–3 orders of magnitude larger than those observed for highly magnetic S-state atoms. This is strong evidence for an additional, dominant, spin relaxation mechanism, electronic interaction anisotropy, in collisions between these "submerged-shell," $L \neq 0$ atoms. These large spin relaxation rates imply that evaporative cooling of these atoms in a magnetic trap will be highly inefficient.

DOI: 10.1103/PhysRevA.81.010702 PACS number(s): 34.50.−s, 32.70.Jz, 37.10.De

Research in cold and ultracold atoms has in recent years increasingly broadened in scope beyond the alkali metal atoms to explore and exploit the diverse range of atomic and chemical properties found across the periodic table. In particular, the lanthanide rare-earth (RE) atoms have attracted considerable experimental and theoretical interest. Recent experiments with RE atoms have resulted in Bose-Einstein condensation of Yb [1], magneto-optical trapping of Er [2] and Dy [3], Zeeman slowing of Tm [4], and large ensembles ($>10^{11}$ atoms) of buffer-gas-loaded and magnetically trapped RE atoms of several species below 1 K [5,6]. This interest in RE systems stems from important, sometimes unique, attributes such as narrow transitions which allow for low Doppler cooling limits and improved frequency standards [7], large magnetic moments with strong long-range dipolar interactions, and a "submerged-shell" character that in certain circumstances can shield atom–atom interactions from anisotropic valence electron shells [6]. Progress with these systems—or any novel atomic system—is dependent on collisional processes, in particular, low rates of inelastic collisions including spin relaxation collisions in trapped samples. Spin relaxation can cause heating as well as drive atoms out of the desired quantum state, thus preventing cooling to lower temperatures and limiting experimental sensitivity and the capacity for new discovery.

Previous experiments and theoretical work with RE atoms, including Er and Tm, revealed suppression of electronic interaction anisotropy in RE–helium collisions. Specifically, in this interaction the anisotropic $4f$ electron distribution was found to be shielded by closed $5s$ and $6s$ electron shells (see [8] and references therein). This submerged-shell nature allowed for sympathetic cooling of RE atoms by cold He and efficient buffer-gas trapping of large numbers of atoms ($>10^{11}$) at millikelvin temperatures. It also explained the reduced collisional frequency broadening of hyperfine clock transitions in Tm [9]. The discovery of efficient shielding and consequent low inelastic rates in the RE–He system gave hope that similar suppression would be found in RE–RE collisions and could allow for efficient evaporative cooling [10]. This could, for example, provide a path to quantum degeneracy for magnetically trapped RE atoms.

In this article, we present measurements of spin relaxation rates in two-body collisions of the trapped submerged-shell species Er ($[\mathrm{Xe}]4f^{12}6s^2$, $^3H_6$) and Tm ($[\mathrm{Xe}]4f^{13}6s^2$, $^2F_{7/2}$), finding them to be very large, in striking contrast to the low rates observed in RE–He systems. These large rates imply an additional spin relaxation mechanism other than spin exchange, dipolar relaxation, and second-order spin-orbit coupling, which are well known from studies with alkali metal atoms. The electrostatic quadrupole–quadrupole interaction is a long-range mechanism for driving inelastic processes in $L \neq 0$ atoms, such as seen in metastable alkaline earth metal systems [11], however, the anisotropic charge distribution in submerged-shell atoms is confined tightly near the nucleus [12]. Thus while the quadrupole–quadrupole interaction is not expected to be shielded, the interaction strength should be far weaker than in outer-shell systems. Although theory has proven very effective for understanding the RE–He system, the current theory of RE–RE cold collisions is incomplete. Despite theoretical developments for understanding collisions of two $L \neq 0$ atoms [13,14], in the RE case these calculations are extremely difficult, and to our knowledge, no theoretical predictions yet exist. Recently, an experiment was done with the transition metal titanium at a temperature of 5 K [15]. Ti has a submerged-shell structure, but the anisotropic Ti $3d$ orbital is larger than the deeply bound RE $4f$ orbital [16], leading to a weaker short-range shielding effect and potentially stronger long-range Ti–Ti interactions [8]. Rapid decay of ^{50}Ti electron spin polarization was observed due to collisions of ^{50}Ti with unpolarized Ti isotopes, but the mechanism of this loss could not be determined because spin relaxation could not be separated from spin exchange. Thus, whether or not submerged-shell atoms exhibit low atom–atom spin relaxation rates remained an open question.

Our experiment is conducted in a double-walled plastic cell maintained at a temperature of ≈500 mK by a superfluid helium heat link to a dilution refrigerator (see Fig. 1). We produce either trapped atomic Er or Tm by laser ablation of solid metal foils into ^{4}He buffer gas in the presence of a magnetic quadrupole field (trap depth, up to 3.7 T) produced by large superconducting anti-Helmholtz coils surrounding the cell. The ablated atoms cool via elastic collisions with the cold buffer gas and, within 50 ms [17], assume a Boltzmann distribution in the trap with a peak density of up to 7×10^{11} cm^{-3}. The trapped cloud is interrogated via laser absorption spectroscopy on the 400.9-nm ($J = 6 \rightarrow 7$) and

 ©2010 The American Physical Society

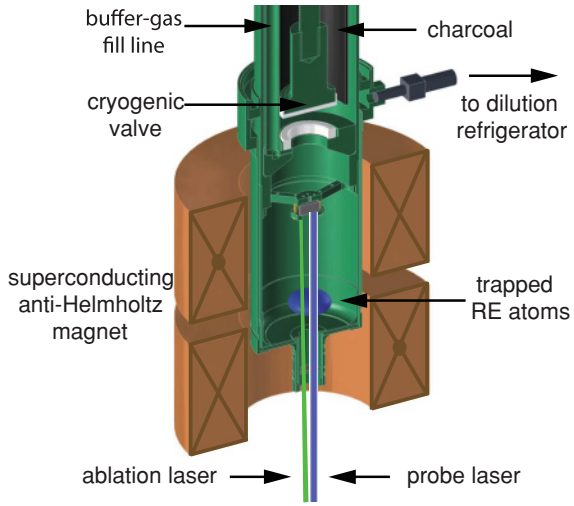

FIG. 1. (Color online) Diagram of the buffer-gas trapping apparatus. A cryogenic valve separates the trapping region of the experimental cell from an additional pumping region and can be used to regulate the buffer-gas density.

415.2-nm ($J = 6 \rightarrow 5$) transitions of Er and on the 409.5-nm ($J = 7/2 \rightarrow 5/2$) transition of Tm.

The amount of buffer gas in the cell is regulated such that the He density is sufficient to cool the atoms after ablation but insufficient to cause significant atom loss from RE–He collisions. This regulation is accomplished by independent control of the cell temperature and the amount of He initially present in the cell. The lack of observed loss from buffer-gas collisions 1 s after ablation implies a He density of less than $10^{12}\,\mathrm{cm}^{-3}$ [17]. Since the observed ablation yield implies a higher initial buffer-gas density, it is likely that heating from the ~5-mJ ablation pulse temporarily desorbs additional He from the cell walls, which readsorbs rapidly. We deliberately maintain a buffer-gas density of about $10^{11}\,\mathrm{cm}^{-3}$ after trap loading to maintain thermal equilibrium between the trapped atoms and the cell.

Example spectra of magnetically trapped Er and Tm are shown in Fig. 2, showing peaks for both Zeeman-broadened $\Delta m_J = \pm 1$ and narrow $\Delta m_J = 0$ transitions. The relative magnitudes of spectral features may be used to estimate the m_J state distribution, however, for the case of a probe laser passing through the trap center the absorption is primarily determined by the total peak atom density rather than the contributions from individual states. Isotope shifts for the 400.9-nm transition of Er were not found in the literature and were determined for nuclear spin-0 isotopes by fitting to spectra measured in zero field at ~4 K. The shifts for isotopes ^{164}Er, ^{168}Er, and ^{170}Er from the ^{166}Er peak are −0.80(4), 0.81(1), and 1.66(2) GHz, respectively.

As noted previously, we ensure that the He density is sufficiently low such that neither elastic nor inelastic RE–He collisional loss is observed (see Fig. 3). The trap loss is then determined by the rate equation:

$$\dot{n}(\vec{r}, t) = -[f_{\mathrm{evap}}(E_{\mathrm{trap}}, T) g_{\mathrm{el}} + g_{\mathrm{in}}] n(\vec{r}, t)^2, \qquad (1)$$

where n is the local density of trapped atoms, and g_{el} and g_{in} are the rate constants for elastic and inelastic atom–atom collisions. The function f_{evap} is the fraction of elastic collisions

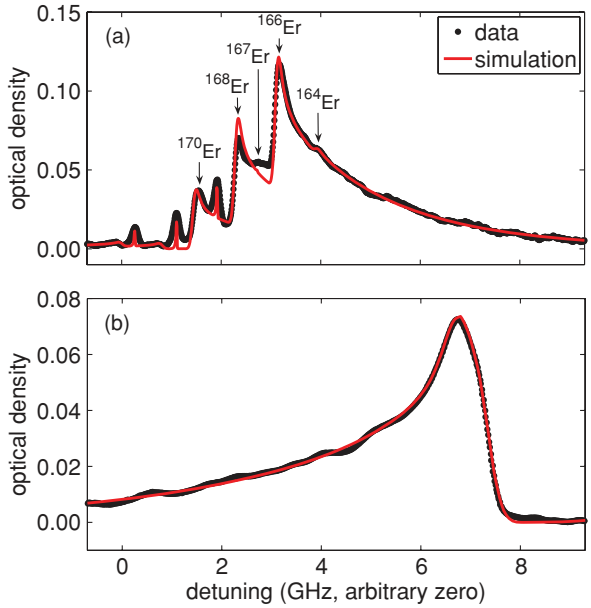

FIG. 2. (Color online) (a) Absorption spectrum of Er on the 400.9-nm ($J = 6 \rightarrow 7$) transition in a 0.99-T-deep (4.6 K) magnetic trap at 530 mK with a peak density of $4.6 \times 10^{10}\,\mathrm{cm}^{-3}$. The $\Delta m_J = +1$ magnetically broadened peaks of the dominant isotopes are labeled. The sharper peaks are $\Delta m_J = 0$ transitions. Hyperfine constants are unknown for the ^{167}Er isotope (23% abundance), and it is ignored in the spectrum simulation. Due to the substantial Zeeman broadening, this does not significantly affect the implied atom density and temperature. (b) Absorption spectrum of Tm on the 409.5-nm ($J = 7/2 \rightarrow 5/2$) transition in a 3.3-T-deep (8.8 K) trap at 500 mK with a peak density of $3.8 \times 10^{11}\,\mathrm{cm}^{-3}$. Tm has a single isotope with $I = \frac{1}{2}$ and known hyperfine splitting [18].

at temperature T that are energetic enough to produce atoms with energy above the trap depth E_{trap} such that the atoms will adsorb on the cold cell walls and be lost from the trap. In our experiments T is low enough that $f_{\mathrm{evap}} < 1\%$ [10], and thus

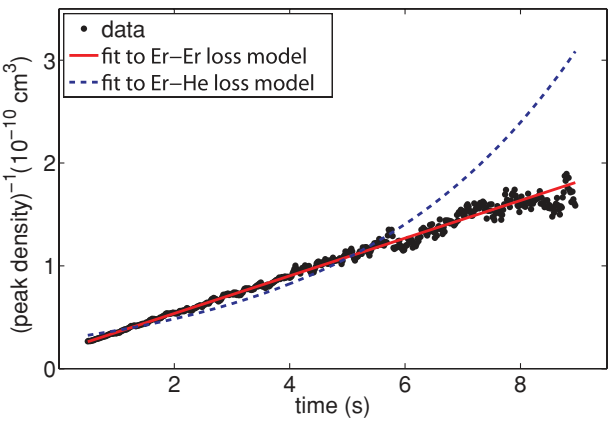

FIG. 3. (Color online) Er decay at 530 mK in a 0.99-T-deep (4.6 K) magnetic trap after ablation at $t = 0$ s. The vertical axis is the reciprocal of the peak atom density obtained from spectra. The solid (red) line is a fit to Eq. (2). The dashed (blue) curve is a fit to the exponential decay expected for collisions with a constant He background. The excellent fit to Eq. (2) ($r = 0.998$) indicates that the atom loss is from Er–Er collisions.

elastic collisions do not contribute significantly to atom loss. Ignoring the first term in Eq. (1), we solve for $n(\vec{r}, t)$, spatially integrate over the trap distribution, and take the reciprocal to reach the simple two-body decay result:

$$\frac{1}{n_0(t)} \equiv \frac{1}{n(r=0,t)} = \frac{1}{n_0(t=0)} + \frac{g_{\rm in} t}{8}. \qquad (2)$$

Plotting n_0^{-1} versus time yields a straight line of slope $g_{\rm in}/8$. Data for Er decay are plotted in this manner in Fig. 3 and fit to Eq. (2). Additionally, a combined fit with free parameters for Er–Er and Er–He collisional loss processes yields a Er–He decay rate consistent with zero, and therefore we conclude that the loss is indeed due to Er–Er collisions.

Fits of atom loss to Eq. (2) yield $g_{\rm in}$ to be $1.5 \pm 0.2 \times 10^{-10}\,{\rm cm}^3\,{\rm s}^{-1}$ for Er and $5.7 \pm 1.5 \times 10^{-11}\,{\rm cm}^3\,{\rm s}^{-1}$ for Tm, with accuracy limited by the density calibration determined from spectra. Both rates are significantly higher than inelastic rates observed for highly magnetic S-state atoms such as Cr, Eu, Mn, and Mo [5,19–22]. The spin relaxation rate constants for these species were measured in similar magnetic traps at similar temperatures and found to be $\lesssim 10^{-12}\,{\rm cm}^3\,{\rm s}^{-1}$, consistent with the magnetic dipole–dipole interaction [8,23] described by

$$V_{\rm dipole}(\vec{r}) = \frac{\mu_0}{4\pi}\frac{\mu^2}{r^3}[(\vec{\mathbf{J}}_1 \cdot \vec{\mathbf{J}}_2) - 3(\vec{\mathbf{J}}_1 \cdot \hat{r})(\vec{\mathbf{J}}_2 \cdot \hat{r})], \qquad (3)$$

where μ is the magnetic moment and r is the distance between two atoms with angular momenta $\vec{\mathbf{J}}_1$ and $\vec{\mathbf{J}}_2$, respectively. The spin relaxation rate constant is dependent on the specific form of the interatomic potential, however, the general μ^4 scaling implied by Eq. (3) provides a relation between dipole-induced inelastic loss rates for atoms of similar electronic structure. Eu ($\mu = 7\mu_B$) and Mn ($\mu = 5\mu_B$), in particular, have a submerged-shell character similar to that of Er ($\mu = 7\mu_B$) and Tm ($\mu = 4\mu_B$).[1] Scaling the cross sections measured for Eu [5] and Mn [22] by μ^4 and averaging yields $g_{\rm in} = 3.4 \times 10^{-13}\,{\rm cm}^3\,{\rm s}^{-1}$ for Er and $g_{\rm in} = 3.5 \times 10^{-14}\,{\rm cm}^3\,{\rm s}^{-1}$ for Tm. The observed inelastic rate constants for Er and Tm in our experiments are 2–3 orders of magnitude larger than these scaled dipolar values, inconsistent with the dipolar loss model and implying another loss mechanism.

A significant fraction of atoms (>20%) in our experiments has $m_J \neq J$, as determined by observing $\Delta m_J = 0$ transitions on the 415.2-nm ($J = 6 \rightarrow 5$) line of Er. Two-body electronic spin exchange collisions will tend to purify the atomic ensemble toward the $m_J = J$ state, but the stability of spectral features with time implies that this is not the case. In addition, since such collisions conserve the total m_J, they cannot cause loss to untrapped states without also populating more strongly trapped states, which would cause an unobserved net increase in absorption. Nuclear spin exchange could lead to trap loss, but observed rates for this process in other submerged-shell atoms with only $I > 0$ isotopes have shown it to be much slower than the loss observed here [5,21]. Hence the observed loss is spin relaxation to untrapped states. In our analysis, we assume $g_{\rm in}$ to be the same for all pairs of atoms of any m_J.

For spin relaxation collisions resulting in a final state with $m_J > 0$, relaxation may not lead immediately to trap loss. In that case, the $g_{\rm in}$ deduced from loss may be smaller than the true spin relaxation collision rate constant, which we call $g_{\rm sr}$. Calculations for collisions between He and $L \neq 0$ atoms such as Tm and O yield larger rates for $\Delta m_J = \pm 1, 2$ transitions than for other transitions, creating effective selection rules [24,25]. Although RE–RE sytems are not theoretically well understood, if such selection rules held in the case of Er, the $m_J = J = 6$ state would on average require several inelastic collisions to reach an untrapped state, contributing to the nonzero $m_J \neq J$ state population noted previously. In addition, collisional energy can promote inelastically colliding atoms to higher m_J states and inhibit loss. These thermal excitations are suppressed for $g_J \mu_B B \gg kT$, however, this condition fails near the trap center where $B = 0$. Considering both these effects, the observed stability of the spectrum suggests that the m_J state distribution achieves a slowly varying balance between loss and excitation. We confirmed this model with simulations of inelastic decay, including thermal excitations and exploring a range of initial m_J state distributions and selection rules. The simulations suggest a ratio $g_{\rm sr}/g_{\rm in}$ of $2.0^{+1.0}_{-0.5}$.

Currently no theoretical predictions for $L \neq 0$ RE–RE spin relaxation rates exist, due to the complexity of the RE electronic structure; however, one reasonable hypothesis to explain the rapid spin relaxation of Er and Tm is that it is induced by electronic interaction anisotropy, as observed in anisotropic outer-shell systems. Experiments with metastable $^3P_2$ states of Ca and Yb have measured inelastic collision rate constants greater than $10^{-11}\,{\rm cm}^3\,{\rm s}^{-1}$ [11,26], nearly as large as the Ca*–Ca* and Yb*–Yb* elastic rate constants. These inelastic rates are similar to those we observe here for Er and Tm atom–atom collisions, suggestive of a complete lack of suppression of electronic interaction anisotropy and in contrast to the dramatic suppression of $>10^4$ observed for spin relaxation collisions with He. It is possible that the unshielded long-range anisotropy of the small RE quadrupole moment is sufficient to cause rapid loss, although multichannel scattering calculations (such as those in [14]) are needed to prove this. Alternatively, the observed RE–RE spin relaxation may be a short-range phenomenon which is unshielded in the RE–RE system due to a much stronger interaction potential than in the RE–He system. In this case, the near-degeneracy of the Born-Oppenheimer potentials corresponding to different projections of the electronic angular momentum onto the internuclear axis could be lifted, causing large inelasticity.

In conclusion, we have measured the loss rate constants for inelastic Er–Er and Tm–Tm collisions and found them to be large. For comparison, the maximum elastic cross section $\sigma_{\rm el}$ in the absence of shape resonances can be derived from the well-known unitarity limit [27]. Using the C_6 coefficient calculated for the Yb–Yb system [28] and assuming elastic collisions between submerged-shell lanthanide RE atoms to be similar, we find the maximum $g_{\rm el} = \sigma_{\rm el}\bar{v} \approx 8 \times 10^{-10}\,{\rm cm}^3\,{\rm s}^{-1}$ at 500 mK. Hence the ratio $g_{\rm el}/g_{\rm sr} \lesssim 10$ for both Er and Tm, implying that evaporative cooling of these atoms in a magnetic

[1]The spin relaxation rate constants for Eu and Mn are consistent with the μ^4 cross-section scaling within experimental error. The same is true between outer-shell Cr and Mo, however, these rates are several times higher.

trap will be highly inefficient [10]. At this temperature we expect ≈40 partial waves to contribute to collisions, and we note that g_{sr} may be different in the ultracold s-wave limit. However, this limit is rather low for these heavy colliding atoms (≈10 μK), so the multi-partial-wave physics will be applicable over a range of experimental conditions.

The large spin relaxation rates for Er and Tm reported here, along with those reported for Ti [15] and recently measured separately for Dy [3,29], represent significant evidence that the submerged-shell character exhibited by roughly a third of the periodic table and responsible for dramatic suppression effects in atom–He collisions does not imply suppression of electronic interaction anisotropy in collisions between $L \neq 0$ atoms. As a result, the highly successful method of evaporative cooling in a magnetic trap may remain confined to (isotropic) S-state atoms. In addition, lifetimes for optically trapped atoms in $L \neq 0$ states may be short due to spin relaxation unless trapped in the absolute ground state. It remains an open question whether interaction anisotropy shielding is unique to collisions with He or whether the RE–RE spin relaxation mechanism is purely long-range and not applicable to collisions between anisotropic RE atoms and S-state atoms, which may preserve the potential for further sympathetic cooling.

We would like to acknowledge numerous helpful discussions with Timur Tscherbul. This work was supported by the National Science Foundation under Grant No. 0757157 and through the Harvard/MIT Center for Ultracold Atoms.

[1] Y. Takasu *et al.*, Phys. Rev. Lett. **91**, 040404 (2003).
[2] J. J. McClelland and J. L. Hanssen, Phys. Rev. Lett. **96**, 143005 (2006).
[3] M. Lu, S. H. Youn, and B. L. Lev, e-print arXiv:0912.0050v2 (2009).
[4] K. Chebakov *et al.*, Opt. Lett. **34**, 2955 (2009).
[5] J. Kim *et al.*, Phys. Rev. Lett. **78**, 3665 (1997).
[6] C. I. Hancox *et al.*, Nature **431**, 281 (2004).
[7] J. L. Hall, M. Zhu, and P. Buch, J. Opt. Soc. Am. B **6**, 2194 (1989).
[8] A. A. Buchachenko *et al.*, Phys. Scr. **80**, 048109 (2009).
[9] E. B. Aleksandrov *et al.*, Opt. Spektrosk. **54**, 3 (1983), [Opt. Spectrosc. **54**, 1 (1983)].
[10] W. Ketterle and N. J. van Druten, Adv. At. Mol. Opt. Phys. **37**, 181 (1996).
[11] D. Hansen and A. Hemmerich, Phys. Rev. Lett. **96**, 073003 (2006).
[12] L. Seijo *et al.*, J. Chem. Phys. **114**, 118 (2001).
[13] R. V. Krems, G. C. Groenenboom, and A. Dalgarno, J. Phys. Chem. A **108**, 8941 (2004).
[14] V. Kokoouline, R. Santra, and C. H. Greene, Phys. Rev. Lett. **90**, 253201 (2003).
[15] M.-J. Lu, V. Singh, and J. D. Weinstein, Phys. Rev. A **79**, 050702(R) (2009).
[16] F. Rakowitz *et al.*, J. Chem. Phys. **110**, 3678 (1999).
[17] C. I. Hancox, Ph.D. thesis, Harvard University, 2005.
[18] A. V. Akimov *et al.*, Quantum Electron. **38**, 961 (2008).
[19] J. D. Weinstein, R. deCarvalho, C. I. Hancox, and J. M. Doyle, Phys. Rev. A **65**, 021604(R) (2002).
[20] S. V. Nguyen, R. deCarvalho, and J. M. Doyle, Phys. Rev. A **75**, 062706 (2007).
[21] J. G. E. Harris, S. V. Nguyen, S. C. Doret, W. Ketterle, and J. M. Doyle, Phys. Rev. Lett. **99**, 223201 (2007).
[22] C. I. Hancox, M. T. Hummon, S. V. Nguyen, and J. M. Doyle, Phys. Rev. A **71**, 031402(R) (2005).
[23] Z. Pavlović, R. V. Krems, R. Cote, and H. R. Sadeghpour, Phys. Rev. A **71**, 061402(R) (2005).
[24] R. V. Krems and A. Dalgarno, Phys. Rev. A **68**, 013406 (2003).
[25] A. A. Buchachenko, G. Chalasinski, M. M. Szczesniak, and R. V. Krems, Phys. Rev. A **74**, 022705 (2006).
[26] A. Yamaguchi, S. Uetake, D. Hashimoto, J. M. Doyle, and Y. Takahashi, Phys. Rev. Lett. **101**, 233002 (2008).
[27] R. Shankar, *Principles of Quantum Mechanics*, 2nd ed. (Plenum Press, New York, 1994), p. 548.
[28] P. Zhang and A. Dalgarno, J. Phys. Chem. A **111**, 12471 (2007).
[29] B. Newman, N. Brahms, Y. S. Au, C. Johnson, C. B. Connolly, J. M. Doyle, D. Kleppner, and T. Greytak (in preparation).